

Evidence against strong correlation in 4d transition-metal oxides CaRuO₃ and SrRuO₃

Kalobaran Maiti* and Ravi Shankar Singh

Department of Condensed Matter Physics and Materials Science, Tata Institute of Fundamental Research, Homi Bhabha Road, Colaba, Mumbai - 400 005, India

(Received 6 August 2004; revised manuscript received 27 January 2005; published 18 April 2005)

We investigate the electronic structure of 4d transition-metal oxides CaRuO₃ and SrRuO₃. The analysis of the photoemission spectra reveals significantly weak electron correlation strength ($U/W \sim 0.2$) as expected in 4d systems and resolves the long-standing issue that arose due to the prediction of large U/W similar to 3d systems. It is shown that the bulk spectra, thermodynamic parameters, and optical properties in these systems can consistently be described using first-principles calculations. The observation of different surface and bulk electronic structures in these weakly correlated 4d systems is unusual.

DOI: 10.1103/PhysRevB.71.161102

PACS number(s): 71.27.+a, 71.10.Fd, 71.20.Be, 79.60.Bm

A Hubbard model consisting of intersite hopping energy t ($\propto W$ =bandwidth) and on-site Coulomb repulsion energy U has been widely accepted as the simplest model to capture correlation effects in the electronic structure. Thus, effective electron correlation strength can be described by a single parameter, U/W ($U/W > 1 \Rightarrow$ insulator, $U/W < 1 \Rightarrow$ metal). Correlation effects in 3d transition-metal oxides (TMOs) have extensively been studied using this model during the past few decades following the discovery of many exotic properties in these systems.¹ Despite the simplicity of the model, the major difficulty arises from large U leading to a nonperturbative nature of the problem, and the presence of various competing effects such as different types of long-range order, interplay between localization and lattice coherence, etc.

4d orbitals in 4d TMOs are more extended than 3d orbitals in 3d TMOs. Thus, correlation effect is expected to be less important in these systems and provide a suitable testing ground for the applicability of various *ab initio* approaches. This is reflected by only a small mass enhancement^{2,3} ($m^*/m_b = 3.0$ in SrRuO₃; m^* =effective mass, m_b =band mass) in the specific-heat measurements. However, photoemission^{4,5} and optical⁶ data reported so far are significantly different from their *ab initio* results. All these studies predict a large U/W similar to that observed in 3d TMOs in contrast to the behavior expected from the highly extended nature of 4d systems. It is thus believed that various approximations (slave boson, techniques in the limit of infinite dimensions, exact calculations for finite-size system, etc.) are necessary to simulate the material properties of these systems. In addition, tetravalent ruthenates have drawn significant attention recently due to the discovery of interesting magnetism,²⁻⁸ unconventional superconductivity,⁹ metal-insulator transitions,¹⁰ etc.

In this paper, we present evidence for weak correlations among 4d TMOs. We report the results of our investigation of the electronic structure of 4d TMOs, SrRuO₃ and CaRuO₃. SrRuO₃ is a ferromagnetic metal. Isostructural and isoelectronic, CaRuO₃ (with a slightly different Ru-O-Ru bond angle; 150° in CaRuO₃ and 165° in SrRuO₃) exhibits antiferromagnetic behavior.^{2,11} Photoemission spectra at different photon energies reveal different electronic structures

for surface and bulk in *both* cases. It is to note here that early 3d TMOs, as well as rare-earth systems, are known to exhibit different surface and bulk electronic structures,¹²⁻¹⁵ which was attributed to an enhancement of U/W at the surface compared to that in the bulk. It was necessary to employ the dynamical mean-field theoretical approach (DMFT) within the limit of an infinite-dimensional Hubbard model to determine the bulk electronic structure in these 3d systems.¹⁶ Interestingly, the bulk spectra in this study could be described remarkably well using *ab initio* approaches. Present results, thus, resolve three fundamental issues in these systems. (a) Electron correlation is significantly weak in 4d TMOs ($U/W \sim 0.2$). (b) First-principles calculations are sufficient to simulate the bulk photoemission and optical responses, and to reproduce m^*/m_b obtained from the specific-heat measurements. (c) The surface and bulk electronic structures can be different even in weakly correlated systems.

High quality polycrystalline samples (large grain size achieved by long sintering at the preparation temperature) were prepared by the solid-state reaction method using ultra-high purity ingredients and characterized by x-ray diffraction (XRD) patterns and magnetic measurements as described elsewhere.^{2,4,11} Sharp XRD patterns reveal pure GdFeO₃ structure with similar lattice constants as observed for single-crystalline samples.² Magnetic susceptibility measurements exhibit a ferromagnetic transition in SrRuO₃ at 165 K and the signature of antiferromagnetic interactions in CaRuO₃ at 180 K. The magnetic moment of 2.7 μ_B in SrRuO₃ and 3 μ_B in CaRuO₃ in the paramagnetic phase is close to their spin-only value of 2.83 μ_B for $t_{2g}^3 t_{2g}^1$ configurations at Ru sites. Photoemission measurements were performed on *in situ* (4×10^{-11} torr) scraped samples^{17,18} using the SES2002 Scienta analyzer at room temperature (paramagnetic phase) in order to avoid complications due to different long-range orders. The experimental resolution was 7 meV, 0.8 eV, and 0.9 eV for measurements with monochromatic He II, Mg $K\alpha$, and Al $K\alpha$ lines.

Valence-band spectra obtained at He II, Mg $K\alpha$, and Al $K\alpha$ excitation energies are shown in Fig. 1. The signature of three discernible features is evident in the figure. While the features appearing at binding energies > 2.5 eV are large in He II spectra, the relative intensity between 2.5 and 0 eV

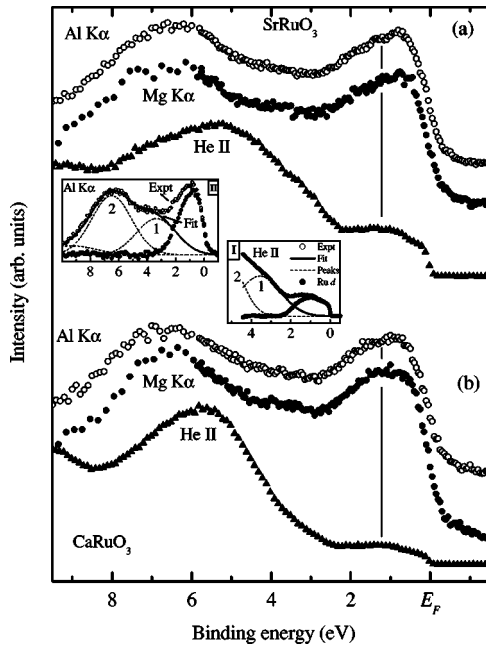


FIG. 1. Valence-band spectra of (a) SrRuO_3 and (b) CaRuO_3 . Subtraction of O $2p$ contributions from He II spectrum of SrRuO_3 is demonstrated in inset (I). Peaks 1 and 2 represent the nonbonding and bonding features. These two peaks are broadened up to XP resolution to obtain O $2p$ contributions in the XP spectrum of SrRuO_3 as shown in inset (II). The relative intensity of the features is obtained by a least-square error method.

binding energies is significantly enhanced in the x-ray photoemission (XP) spectra. Considering strong dependence of the relative transition matrix elements on excitation energies,¹⁹ the 0–2.5 eV can be attributed to essentially Ru $4d$ electron excitations with the O $2p$ contributions appearing beyond 2.5 eV.

In order to understand these results, we calculated the electron density of states (DOS) of CaRuO_3 and SrRuO_3 using full-potential linearized augmented plane-wave method (FLAPW) within the local-density approximations (LDA) for the experimentally obtained crystal structure in the paramagnetic phase.²⁰ The convergence was achieved using 512 k points within the first Brillouin zone. Total DOS (TDOS) and partial DOS (PDOS) corresponding to Ru $4d$ and O $2p$ states are shown in Fig. 2. No significant contribution from Ca and Sr states are observed in this energy range. Three distinct groups of peaks are evident in the figure in the occupied part. Nonbonding O $2p$ states appear between 2–4 eV and the bonding states with dominant O $2p$ contributions appear at higher binding energies. This is also manifested in Fig. 1 by an enhancement in intensity at 7 eV in the XP spectra compared to the He II spectra. He II spectra exhibit a peak below 6 eV. The intensity at E_F arises primarily due to Ru $4d$ split t_{2g} bands. The broad and empty e_g bands appear beyond 1-eV above E_F .

Small distortion of RuO_6 octahedra lifts the degeneracy of the t_{2g} band as shown in the insets of Fig. 2. While the d_{xy} , d_{yz} , and d_{xz} bands in SrRuO_3 have similar width ($W = 2.4$ eV), the total bandwidth is about 3.1 eV due to the splitting of the t_{2g} band. In CaRuO_3 , the total bandwidth is

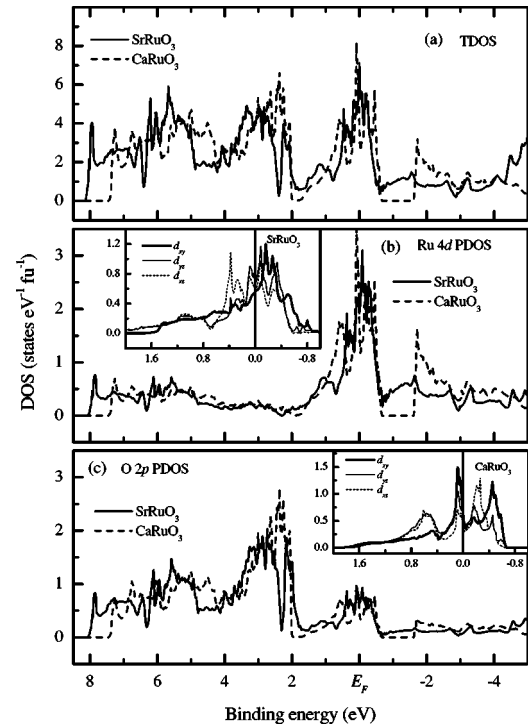


FIG. 2. (a) TDOS, (b) Ru $4d$ PDOS, and (c) O $2p$ PDOS in SrRuO_3 and CaRuO_3 . d_{xy} , d_{yz} , and d_{xz} bands are shown in the inset in (b) for SrRuO_3 and in (c) for CaRuO_3 .

about 2.4 eV. Interestingly, the widths of the d_{xy} , d_{xz} , and d_{yz} bands vary between 2.3–2.4 eV, which is similar to those in SrRuO_3 . This reveals that the small change in Ru-O-Ru bond angle between SrRuO_3 and CaRuO_3 has essentially no influence on W (the bandwidth of the individual d bands) and thus, U/W in these systems. The center of mass for the d_{xy} band appears very close to E_F in both cases, while the d_{xz} and d_{yz} bands appear at lower energies.

It is now clear that the feature close to E_F has primarily Ru $4d$ character. High resolution in the He II spectra leads to a minimal overlap between the O $2p$ and Ru t_{2g} bands (see Fig. 1). Hence, it is possible to delineate Ru t_{2g} contributions quite reliably by subtracting the O $2p$ tail as shown in the inset (I) of Fig. 1 for SrRuO_3 . Ru t_{2g} bands, thus extracted for both CaRuO_3 and SrRuO_3 , are shown in Fig. 3(a). Large intensity at E_F represents the extended states as also seen in the band-structure calculations and is commonly known as a “coherent feature.” Interestingly, the maximum intensity appears around 1.2 eV as observed before,^{4,5} while the theoretical intensity peaks at about 0.5 eV with negligible contributions beyond 1 eV [see Fig. 3(b)]. Thus, this feature is often attributed to the signature of the electronic states essentially localized due to electron correlations and is termed as an “incoherent feature.” Spectral modifications observed in Fig. 3(a) indicate larger correlation effects in CaRuO_3 compared to SrRuO_3 as predicted from the structure. While large intensity at E_F indicates metallic character, the complete dominance of this apparent incoherent feature was taken as evidence of the presence of strong correlation effects in previous studies.^{4–6} We present our results below, establishing that this feature essentially arises due to the contributions from the surface electronic structure.

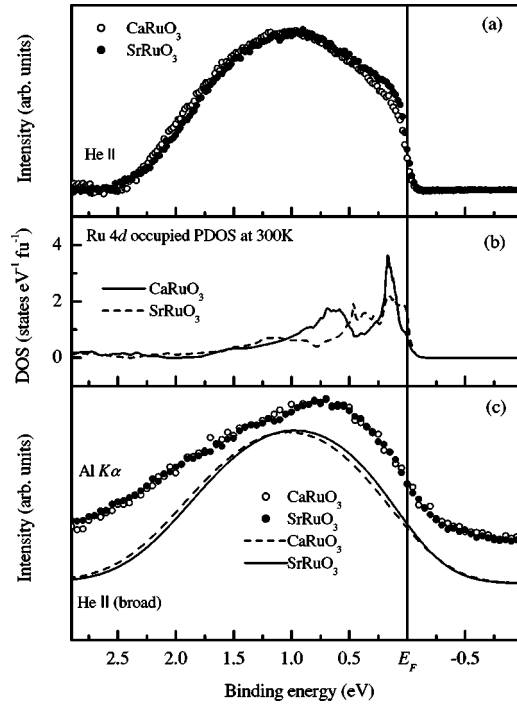


FIG. 3. (a) Ru t_{2g} band extracted from He II spectra for CaRuO₃ and SrRuO₃. (b) Ru $4d$ PDOS convoluted with Fermi distribution function at 300 K. This represents the signature of coherent feature. (c) Ru t_{2g} band extracted from XP spectra for CaRuO₃ and SrRuO₃. The resolution-broadened He II spectra are also shown for comparison.

Interestingly, the XP spectra in Fig. 1 exhibit highest intensity at 0.5 eV for the Ru $4d$ band even though the intensities at higher energies contain contributions from resolution-broadened O $2p$ band tails. In order to subtract these contributions from the XP spectra, we broadened peaks 1 and 2 in inset (I), representing the O $2p$ features in the He II spectra up to the resolution broadening of the XP measurements, and the relative intensities of features 1 and 2 were obtained *via* a least-square error fit. The subtracted spectra shown in Fig. 3(c) clearly possess different line shape compared to the solid lines representing resolution-broadened He II spectra. The x-ray photoelectrons has a significantly larger escape depth compared to the ultraviolet photoelectrons, which leads to a significantly larger bulk sensitivity in XP spectroscopy compared to that in ultraviolet photoemission spectroscopy at 40.8 eV. Thus, it is obvious that the bulk and surface electronic structures are significantly different in these systems. *We do not observe any change in line shape of the t_{2g} band in the XP spectra of CaRuO₃ and SrRuO₃ as expected from the band-structure results described above.*

Photoemission intensity can be expressed as $I(\epsilon) = [1 - e^{-d/\lambda}]f^s(\epsilon) + e^{-d/\lambda}f^b(\epsilon)$, where d is the thickness of the surface layer and λ is the escape depth of the photoelectrons. $f^s(\epsilon)$ and $f^b(\epsilon)$ represent the surface and bulk spectral functions, respectively. Since d and λ are expected to change in the same way due to the difference between $3d$ and $4d$ sites, experimentally estimated d/λ values in a similar system CaSrVO₃ (Ref. 12) are a good approximation to extract $f^s(\epsilon)$

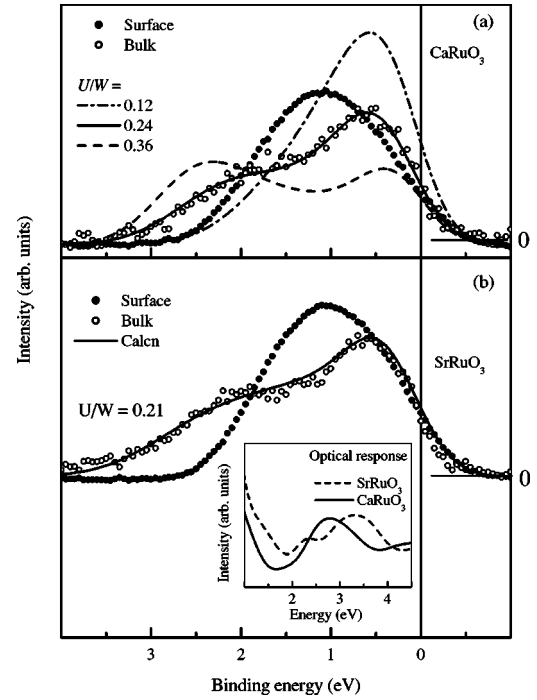


FIG. 4. Surface and bulk spectra in (a) CaRuO₃ and (b) SrRuO₃. The solid lines represent the simulated spectra from first-principles calculations. The dashed and dot-dashed lines in (a) represent the simulated spectra for $U/W=0.12$ and 0.36 , respectively. The calculated optical response is shown in the inset. The line shape is found to be similar to that observed experimentally (Ref. 6).

and $f^b(\epsilon)$ in these systems. We observe that a change in d/λ values by more than 10% leads to unphysical intensities providing confidence in this procedure. The extracted $f^s(\epsilon)$ and $f^b(\epsilon)$ are shown in Fig. 4. $f^s(\epsilon)$ in both the cases is dominated by the intensity centered at 1 eV. $f^b(\epsilon)$ exhibit a large coherent feature with the peak at about 0.5 eV as observed in the *ab initio* calculations. The feature around 2 eV indicates the presence of some degree of correlation effects, which is estimated below.

The spectral function can be expressed as $f^b(\epsilon) = -1/\pi \text{Im}\Sigma_k G_k(\epsilon)$, where $G_k(\epsilon)$ is the retarded Green's function representing the many-electron system and is given by $G_k(\epsilon) = 1/(\epsilon - \Sigma_k(\epsilon) - \epsilon_k)$. $\Sigma_k(\epsilon)$ is the self-energy of the system. For small U , $\Sigma_k(\epsilon)$ can be calculated using a perturbation approach up to the second-order term²¹ within the local approximations. We have used Ru t_{2g} PDOS for these calculations. The calculated spectral functions are shown by solid lines in Fig. 4. The fit to the experimental spectra is remarkable. Most interestingly, U/W is found to be significantly small (0.24 for CaRuO₃ and 0.21 for SrRuO₃; $U=0.6\pm 0.05$ eV in both cases) in sharp contrast to all previous predictions.⁴⁻⁶ A small variation in U/W leads to significantly large spectral weight transfer as shown in Fig. 4(a). We calculated the mass enhancement factor following the relation, $m^*/m_b = 1 - \partial/\partial\epsilon[\text{Re}\Sigma(\epsilon)]|_{\epsilon=E_F}$. Interestingly, m^*/m_b for SrRuO₃ is almost the same ($=2.9$) as that obtained ($=3.0$) from specific-heat measurements. While U/W in CaRuO₃ is a little larger than that in SrRuO₃, m^*/m_b in CaRuO₃ is found to be close to SrRuO₃ and somewhat smaller than its experimental value.

It is important to realize here that the optical response (particularly in transmission mode) corresponds essentially to the bulk electronic structure.⁶ Thus, the description of weak correlation effects in the bulk electronic structure should also be reflected in the optical spectra. We thus calculated the optical response by calculating the joint density of states using the WIEN program.²⁰ The calculated spectra (correlation effects are not considered) shown in the inset of Fig. 4(b) resemble the experimental spectra by Ahn *et al.*⁶ remarkably well. *This study, thus, establishes that these weakly correlated 4d TMOs provide a model system for the applicability of the first-principles approaches in determining the thermodynamic, optical, and spectroscopic properties.*

Differences in the surface and bulk electronic structures in 3d TMOs, as well as in rare earths, were attributed to the enhancement of U/W due to the band narrowing at the surface.^{12,16} Thus, the observation of different $f^s(\epsilon)$ and $f^b(\epsilon)$ in these weakly correlated 4d TMOs is unusual. Most surprisingly, the surface peak appears at lower binding energies than the incoherent peak in the bulk spectra. It is observed

that small distortion of RuO_6 octahedra in the orthorhombic structure lifts the degeneracy of the bulk t_{2g} band (see insets in Fig. 2). Whether the surface layer consists of Sr/Ca-O or Ru-O layer, the absence of periodicity along the surface will enhance this distortion leading to a different crystal-field symmetry presumably close to D_{4h} symmetry ($t_{2g} \Rightarrow e_g + b_{2g}$); where d_{xz} and d_{yz} bands exhibit e_g symmetry and the d_{xy} band has b_{2g} symmetry.¹⁴ Thus, the peak around 1 eV in the surface spectra may be attributed to an essentially filled e_g band with the b_{2g} band appearing above E_F .

In summary, correlation effects are found to be significantly weak in these 4d systems. This resolves the long-standing issue that arose due to the prediction of large electron correlation in these systems similar to 3d TMOs. We find that the photoemission and optical responses, and thermodynamic parameters, can be consistently described within the first-principles approaches. The observation of different surface electronic structure in these weakly correlated 4d systems may possibly be attributed to the change in symmetry at the surface.

*Electronic address: kbmaiti@tifr.res.in

- ¹A. Georges, G. Kotliar, W. Krauth, and M. J. Rozenberg, *Rev. Mod. Phys.* **68**, 13 (1996); M. Imada, A. Fujimori, and Y. Tokura, *ibid.* **70**, 1039 (1998).
- ²G. Cao, S. McCall, M. Shepard, J. E. Crow, and R. P. Guertin, *Phys. Rev. B* **56**, 321 (1997).
- ³P. B. Allen, H. Berger, O. Chauvet, L. Forro, T. Jarlborg, A. Junod, B. Revaz, and G. Santi, *Phys. Rev. B* **53**, 4393 (1996).
- ⁴J. Okamoto, T. Mizokawa, A. Fujimori, I. Hase, M. Nohara, H. Takagi, Y. Takeda, and M. Takano, *Phys. Rev. B* **60**, 2281 (1999).
- ⁵J. Park, S. J. Oh, J. H. Park, D. M. Kim, and C. B. Eom, *Phys. Rev. B* **69**, 085108 (2004).
- ⁶J. S. Ahn, J. Bak, H. S. Choi, T. W. Noh, J. E. Han, Y. Bang, J. H. Choi, and Q. X. Jia, *Phys. Rev. Lett.* **82**, 5321 (1999).
- ⁷I. I. Mazin and D. J. Singh, *Phys. Rev. B* **56**, 2556 (1997).
- ⁸P. A. Cox *et al.*, *J. Phys. C* **16**, 6221 (1983); F. Fukunaga and N. Tsuda, *J. Phys. Soc. Jpn.* **63**, 3798 (1994).
- ⁹Y. Maeno *et al.*, *Nature (London)* **372**, 532 (1994).
- ¹⁰A. W. Sleight and J. L. Gillson, *Mater. Res. Bull.* **6**, 781 (1971).
- ¹¹R. S. Singh, P. L. Paulose, and K. Maiti (unpublished).
- ¹²K. Maiti *et al.*, *Europhys. Lett.* **55**, 246 (2001).
- ¹³K. Maiti, P. Mahadevan, and D. D. Sarma, *Phys. Rev. Lett.* **80**, 2885 (1998); K. Maiti and D. D. Sarma, *Phys. Rev. B* **61**, 2525 (2000).
- ¹⁴K. Maiti, A. Kumar, D. D. Sarma, E. Weschke, and G. Kaindl, *Phys. Rev. B* **70**, 195112 (2004).

- ¹⁵C. Laubschat, E. Weschke, C. Holtz, M. Donke, O. Strebler, and G. Kaindl, *Phys. Rev. Lett.* **65**, 1639 (1990); L. Z. Liu, J. W. Allen, O. Gunnarsson, N. E. Christensen, and O. K. Andersen, *Phys. Rev. B* **45**, 8934 (1992).
- ¹⁶A. Liebsch, *Phys. Rev. Lett.* **90**, 096401 (2003); E. Pavarini, S. Biermann, A. Poteryaev, A. I. Lichtenstein, A. Georges, and O. K. Andersen, *ibid.* **92**, 176403 (2004).
- ¹⁷Since perovskite structure has no cleavage plane, scraping has a sufficiently high probability to expose intrinsic bulk material through intragrain fracture [Susaki *et al.*, *Phys. Rev. Lett.* **78**, 1832 (1997)]. We have verified this on a similar system, SrVO_3 . We find that the spectra collected from scraped and cleaved single crystals are identical [K. Maiti *et al.* (unpublished)].
- ¹⁸A small impurity contribution could not be avoided as that also observed in the high quality films studied recently (Ref. 5). Reproducibility of the spectra was confirmed after every scraping cycle.
- ¹⁹J. J. Yeh and I. Lindau, *At. Data Nucl. Data Tables* **32**, 1 (1985).
- ²⁰P. Blaha, K. Schwarz, G. K. H. Madsen, D. Kvasnicka, and J. Luitz, WIEN2K, *An Augmented Plane Wave + Local Orbitals Program for Calculating Crystal Properties* (Karlheinz Schwarz, Techn. Universität Wien, Austria, 2001).
- ²¹G. Treglia *et al.*, *J. Phys. (Paris)* **41**, 281 (1980); *Phys. Rev. B* **21**, 3729 (1980); D. D. Sarma, F. U. Hillebrecht, W. Speier, N. Martensson, and D. D. Koelling, *Phys. Rev. Lett.* **57**, 2215 (1986).